JACS
JOURNAL OF THE AMERICAN CHEMICAL SOCIETY

Article

pubs.acs.org/JACS

Localized Reaction at a Smooth Metal Surface: *p*-Diiodobenzene at Cu(110)

Lydie Leung, Tingbin Lim, Zhanyu Ning, and John C. Polanyi*

Lash Miller Chemical Laboratories, Department of Chemistry and Institute of Optical Science, University of Toronto, 80 St. George Street, Ontario M5S 3H6, Canada

Supporting Information

ABSTRACT: Halogenation at a semiconductor surface follows simple dynamics characterized by "localized reaction" along the direction of the halide bond being broken. Here we extend the study of halide reaction dynamics to the important environment of a smooth metal surface, where greater product mobility would be expected. Extensive examination of the physisorbed reagent and chemisorbed products from two successive electron-induced reactions showed, surprisingly, that for this system product localization and directionality described the dynamics at a metal. The reagent was *p*-diiodobenzene on Cu(110) at 4.6 K. The first C−I bond-breaking yielded chemisorbed iodophenyl and I-atom(#1), and the second yielded phenylene and I-atom(#2). The observed collinear reaction resulted in secondary encounters among products, which revealed the existence of a surface-aligned reaction. The molecular dynamics were well explained by a model embodying a transition between an *a priori* ground state and a semiempirical ionic state, which can be generally applied to electron-induced chemical reactions at surfaces.

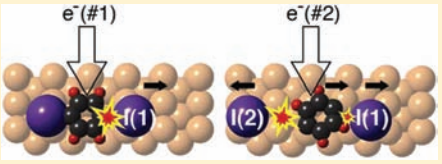

INTRODUCTION

Scanning tunneling microscopy (STM) opens the way to the study of surface reactions, one molecule at a time.[1−4] For semiconductor surfaces the molecular reaction dynamics have been inferred from the distance and direction that the newly formed products travel away from the reagent; the most favored distance of travel is to a surface site adjacent to the reagent molecule, leading to the description "localized atomic reaction" (LAR).[5−8] The prevalence of LAR at semiconductor surfaces has been exploited as a means to the "molecular-scale imprinting" of self-assembled patterns, using light, heat, or electrons to induce the localized reaction.[9,10] The localization in LAR has been attributed to the lowering of the reaction barrier for concurrent bond extension in the old bond being broken and the new bond being formed, only possible in a localized event.[5,11] The favored direction of motion of the reacting halogen atom in the photo-halogenation[6] and thermal halogenation[12] of a silicon substrate by 1,2- and 1,4-dihalobenzenes[6] and dihaloxylenes[12] involved linear extension of the C−X bond. Electron-induced surface chlorination of silicon by chlorobenzene has been studied in detail by Palmer, Sloan, and co-workers who showed that, though LAR and directed C−X bond-rupture were prevalent near threshold, the spread in distance and direction of the reacting Cl increased with increasing energy.[13,14]

Similar considerations might suggest that localization of reaction would dominate even at metal surfaces, which are much smoother than a semiconductor. The evidence has until now been sparse. The halogenation of copper surfaces by halobenzenes is, nonetheless a much studied process since it constitutes the first step in the Ullmann reaction[15] for synthesizing biaryls. In a pioneering study, Rieder and co-workers simulated the Ullmann reaction for iodobenzene on Cu(111) under a scanning tunneling microscope tip at 20 K.[16] In an early study of the dynamics of *p*-diiodobenzene on Cu(111) performed in the Weiss laboratory,[17] the reaction took place at room temperature and subsequently the outcome was examined by STM at 77 K. The finding was that the two liberated I-atoms were sufficiently mobile at the surface to move toward one another to ∼4 Å from a separation of 7.2 Å in the parent molecule. The initial location of the newly formed I-atoms were not obtainable. Extensive studies have been made of the polymerization of the phenylene product.[18,19] For iodobenzene on Cu(110) head-to-head (opposed I-atom) dimer formation was reported by Dougherty et al.[20] at ∼100 K; they too observed mobility in the phenyl and I-atom electron-induced reaction products. By reducing the surface temperature at Au(111) to <10 K for the case of CH_3SSCH_3(ad) Maksymovych and Yates[21] observed both localized and directed electron-induced reaction, with conformation retention in the two CH_3S fragments. More recently this laboratory reported on the electron-induced iodination of Cu(110) at 4.6 K by a family of four linear polymers of *p*-diiodobenzene,[22] $(pDIB)_n$, varying in I···I length from 7 to 29 Å; these reacted in each case to give I−Cu imprints 7.2 Å farther apart (not closer together as in ref 17) than the initial separation. The two C−I bonds could in many cases be observed in the current vs time plots to be broken sequentially by two impacting electrons, but only the final result of the double-dissociation was recorded. The uniform increase in separation between the pair of chemisorbed I-atoms down the

Received: February 17, 2012
Published: May 7, 2012

   dx.doi.org/10.1021/ja301608q | *J. Am. Chem. Soc.* 2012, 134, 9320−9326

series of polymers $(pDIB)_n$ was consistent with localized and directed reaction in each case.

Missing, for metals, was the important information concerning the dynamics of the individual bond-breaking events which have not previously been investigated. These are examined in the present detailed study of the monomer pDIB using a combination of STM measurements and density functional theory (DFT)-based molecular dynamics (MD) simulation. In the first bond-breaking event, iodophenyl (IPh) and I-atom(#1), we find recoil in opposite directions along [001] of the underlying copper; in the second event, phenylene (Ph′) and I-atom(#2) are found to recoil in opposite direction along the same axis. Analysis at this level of detail, while confirming the overall 7.2 Å increase in I···I separation measured at the surface, shows that the initial localization of the I-atom (#1 or #2) is to a substantially shorter distance, 1.8−2.7 Å from its original site in the parent molecule or radical, commensurate with highly localized reaction. The final I···I separation has additional contributions from the recoil of the I-atom(#2) while still bound to IPh, and an instructive further contribution to the relocation of I-atom(#1) in a secondary encounter with Ph′. This secondary encounter has the properties of "surface-aligned reaction" (SAR),[23−35] not previously observed at the atomic level, which, due to favorable alignment and impact parameter in this instance invariably displaces the chemisorbed I-atom(#1) by a one lattice constant of 3.6 Å to a specific further chemisorbed site along [001].

The analysis of the reaction, with its alternative pathways, is well explained by DFT-based calculations involving MD on a semiempirical pseudopotential electronically excited energy surface, and thereafter on a neutral ground state.

METHODS

STM Experiments. All experiments were performed in a low-temperature ultrahigh vacuum scanning tunneling microscope (Omicron), with a base pressure of $<3.0 \times 10^{-11}$ mbar. STM images were recorded in the constant current mode at 4.6 K. The Cu substrate was cleaned by repeated cycles of Ar^+ bombardment (0.6 keV, 7 μA) followed by annealing at 800 K, until no contamination could be detected by STM. *p*-Diiodobenzene (99%) was dosed from a capillary tube directed at the copper crystal. The crystal reached a maximum temperature of 7.8 K during dosing. Dissociation of the C−I bond was electron-induced by placing the STM tip over the middle of the pDIB or IPh feature and maintaining a constant bias voltage, 1.40 V for the first electron-induced reaction and 1.60 V for the second, with the feedback current disabled, for up to 1 s. The electron order for the breaking of both C−I bonds was determined by varying the tunneling current at the threshold voltage of +1.40 and +1.60 V for the first and second C−I bonds, respectively.

Theory. Theoretical simulations, including the ground-state of the physisorbed pDIB molecule, the products of the two electron-induced reactions, nudged elastic band calculation of minimum energy path for reaction, and the electron-induced MD trajectories, were obtained using the Vienna Ab-initio Simulation Package (VASP),[36] including a semiempirical van der Waals' correction.[37] The electronic structures were calculated through a generalized gradient approximation using the Perdew−Burke−Ernzerhof functional[38] with projector augmented waves (PAW). The surface Brillouin zones of the system were sampled using the gamma point only. The supercell (8×4) consisted of 160 copper atoms in five layers, and a vacuum gap of at least 15 Å. The adsorbates were placed with the plane of the benzene ring parallel to the surface at a distance of initially 3 Å above the surface of the copper. All atoms in the adsorbates and the first three layers of copper were allowed to relax until the force on each atom was less than 0.01 eV/Å. The STM image simulations were generated by bSKAN[39] using the calculated wave functions of the initial and final states from VASP.

An ionic PAW pseudopotential approach[40] was implemented to simulate the electron attachment that led to formation of a molecular anion. The ionic pseudopotential was constructed by taking electrons from an inner core shell to the valence shell. To generate an ionic pseudopotential for I^- rather than taking the real ionic configuration $[Kr]4d^{10}5s^25p^6$, we used the ionic configuration $[Kr]4d^95s^25p^6$ in which an electron from the 4d shell was placed into the valence shell 5p (ref 41). This ionic pseudopotential approach provides a satisfactory description of the valence wave function, and hence the chemical bonding (see details in Supporting Information). We have included an image charge while calculating the ionic state. The image charge was simulated by assuming that the ionic charge is a point charge Q on top of the copper surface at a distance d. Here, d is determined by the position of the anionic atom, which is calculated in each MD step. Hence, the image charge $-Q$ is under the surface at a distance d. The force due to the image charge is $F = -Q^2/(16\pi\varepsilon_0 d^2)\mathbf{z}$, and the correction of total energy is $E_{image} = -Q^2/(8\pi\varepsilon_0 d)\mathbf{z}$, where $\mathbf{z}$ is the surface normal vector.

The first-principles MD simulations were performed by solving the equations of motion while preserving the number of atoms (N), the volume of the system (V), and the total energy (E). The conservation of total energy was achieved by using a small time step. For the MD simulations, a time step of 0.5 fs was used, which gave an average drift of the total energy of less than 0.01 eV/ps. The forces on the ions were calculated at each time step using the Hellmann−Feynman theorem as implemented in VASP.

Modeling of the electron-induced reaction of the second C−I bond was similar to the first. In this case unit negative charge was added to the antibonding orbital of the single C−I bond of the IPh residue from the first bond-break. A minimum time of 70 fs on the ionic potential energy surface (PES*) was required for the reaction to occur after reversion to the ground-state potential energy surface (PES). The MD simulation gave information regarding paths A and B for second C−I bond-breaking to yield A′ and B′. For both paths A and B, when the second electron released I-atom(#2) to the left along $[00\bar{1}]$, the model showed it moving linearly to the first four-fold hollow.

RESULTS AND DISCUSSION

First C−I Bond Dissociation. As previously reported,[22] *p*-diiodobenzene (pDIB) physisorbs with its phenyl ring flat on the Cu(110) surface at 4.6 K. It is imaged as an oval protrusion with its long axis parallel to the [001] direction. The long axis corresponds to the I···I axis, with the I-atoms of pDIB resting on short bridge sites of the copper surface. Its physisorption energy is −1.10 eV (see Supporting Information). An experimental STM image of the physisorbed pDIB and a simulated image of the calculated physisorption geometry (see Methods) are shown in Figure 1a.

We have examined 117 cases of C−I-atom(#1) bond dissociation in physisorbed pDIB induced by electrons tunneling from the STM tip to the surface, to obtain the initial chemisorbed product distribution at 4.6 K of I-atom and IPh. Under these conditions, only the first of the two C−I bonds on the physisorbed pDIB molecule was broken, forming an I-atom and an IPh residue, leading to two principal final states by the pathways designated A and B in Figure 1b,c.

Path A is distinguished from path B by the fact that in path A the IPh shows minimal recoil. This difference in recoil distance corresponds to the fact that the IPh binds to a Cu-atom closely adjacent to its original location as pDIB in path A (see Cu-1, circled in Figure 1b), and to the next adjacent Cu-atom along [001] in the case of path B (Cu-2, Figure 1c).

Paths A and B account for 50 and 33%, respectively, of the 117 cases examined. In addition two other minor reaction paths, C (10%) and D (7%), were observed. In paths C and D the recoiling IPh could be seen in the STM image to have

dx.doi.org/10.1021/ja301608q | J. Am. Chem. Soc. 2012, 134, 9320−9326

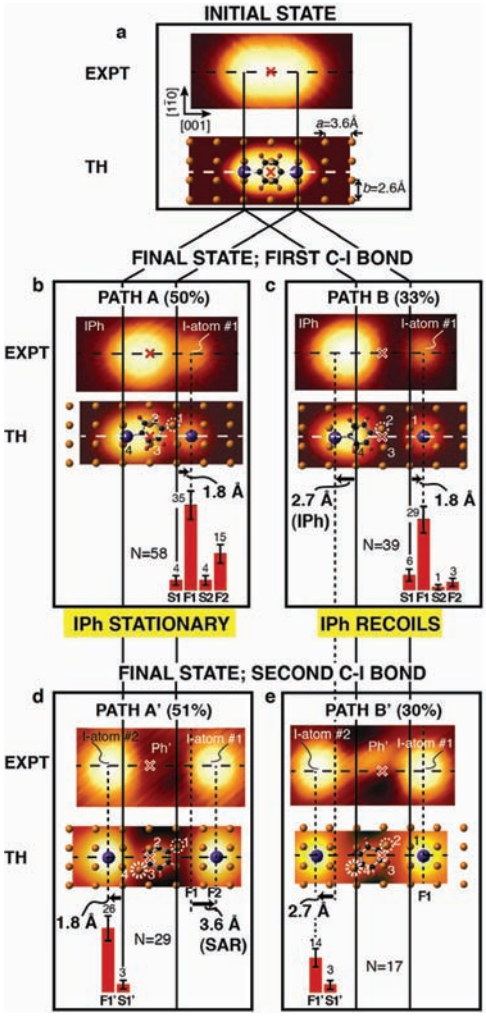

Figure 1. Dissociation of first and second C−I bonds. (a) Initial state images, experiment (EXPT) and theory (TH), for pDIB on Cu(110). The center of the molecule is indicated by the red cross. The molecule has its long I···I axis along the [001] direction (dashed line). The solid vertical lines correspond to the position of the I-atoms in the physisorbed pDIB molecule *prior* to reaction. (b,c) Location of the products of the first electron-induced reaction for paths A and B. The first I-atom's (#1) distributions along the [001] direction are indicated by two histograms. The first I-atom, #1, occupies mainly the closest four-fold hollow site (F1). The iodophenyl (IPh) in path A is almost stationary; the location of the C−Cu bond is marked by a dashed circle at Cu-1. In path B, the IPh recoils by 3.2 Å and its point of attachment to the surface, Cu-2 is circled. (d,e) Locations of the products, I-atom(#2) and phenylene (Ph′), from the second electron-induced reaction. The distributions of the second I-atom (#2) show that its preferred site for paths A′ and B′ is the closest four-fold hollow (F1′). In path A′ the Ph′ is bound to the surface at Cu-1 and Cu-3. The C−Cu bonds in the case of path B′ are marked by the dashed circles at Cu-2 and Cu-4. The difference between outcomes A′ and B′ consists in the fact that in A′ the Ph′ is closer to I-atom(#1) than I-atom(#2), whereas in B′ it is symmetrically placed between the I-atoms. For all states, the calculated STM simulations (labeled TH) shown beneath a diagram of the molecular geometry used, are in good agreement with the experimental images. All STM images were obtained at I = 0.5 nA and V_s = +1.0 V.

rotated significantly in the plane of the surface, away from the [001] axis. In path C this rotation amounted to ∼45° and in path D to 125°. These minor pathways are illustrated by STM images in Figure S1 in the Supporting Information. Our modeling of the dynamics included the first and second C−I bond-breakings for pathways A and B.

The direction of recoil of I-atom(#1) is clearly seen to be along [001], which is the direction of the C−I bond prior to dissociation. In the two major pathways, A and B (as also in pathway C, Figure S1), the first I-atom moving to the right in Figure 1b and c, binds predominantly to chemisorb at the first four-fold hollow. The displacement of the I-atom in going from the physisorbed to the chemisorbed state by pathways A, B, and C (totaling 98% of the reaction) is by 1.8 Å. This is the highest possible degree of "localization" of the product to the neighborhood of the reagent. By contrast, in the minor pathway D the first I-atom was found exclusively in the second four-fold hollow site. This exceptional outcome could be due to the observed high degree of rotation in the newly formed IPh which can bring its I-atom(#2) into the proximity of the departing I-atom(#1), which then gains energy by way of a "secondary encounter". The breaking of the second C−I bond in pathway A will be shown below to lead to an unequivocal example of a "secondary encounter".

Second C−I Bond Dissociation. At a higher bias voltage of +1.6 V, the second C−I bond in IPh broke to liberate I-atom(#2). The objective, again, was to observe the initial product distribution, in this case in I-atom(#2) and in the Ph′ residue. Both these products bound chemically to the copper surface. We examined a total of 58 second-bond-breaking reactions. The reaction products for paths A and B of Figure 1 constitute two of the possible *reagents* for second-bond-breaking. The product distributions that result from second-bond-breaking are shown below in panels d and e of Figure 1, labeled A′ and B′. Further second-bond-breaking reactions originated in paths C and D (Figure S1) and are shown as C′ and D′ (Figure S1d,e) directly below the reagents for the second-bond-breaking in that figure. Breaking the second C−I bond (as for the first, which moved along [001] to the right of Figure 1), the I-atom recoiled along the prior direction of the reagent C−I bond (this time to the left along [00$\bar{1}$]).

We now outline the dynamics for the second-bond-breaking. In the case in which Figure 1b gives the reagent for the second-bond-breaking and Figure 1d the product (A→A′) the second I-atom coming this time from a largely non-recoiling IPh chemisorbed at the closest four-fold hollow, F1, while the Ph′ turned so as to attach to Cu-1 and 3. This turning (see later) caused a secondary encounter of Ph′ with I-atom(#1). Comparison of Figure 1b with Figure 1d below shows that I-atom # 2 has reacted locally by motion to the left by 1.8 Å along [00$\bar{1}$]. At the same time the Ph′ has tilted to the right displacing the product of the first-bond-breaking, I-atom(#1), to the right along [001] by 3.6 Å. This "secondary encounter" will be described in more detail below, with the aid of our dynamical model.

Path B→B′ (Figure 1c,e) constitutes a less frequently observed route for second-bond-breaking. As before, the *reagent* for second-bond-breaking is the product of first-bond-breaking, i.e., Figure 1c. The C−I bond that yields I-atom(#2) is in an IPh that has recoiled to the left ([00$\bar{1}$]) by 2.7 Å, carrying its I-atom to a point short of the nearest Cu short-bridge. As a consequence I-atom(#2) in reacting at a four-fold hollow travels a further 2.7 Å from its former position in the IPh′ (Figure 1e). The Ph′ chemisorbs at Cu-2 and Cu-4 (circled in Figure 1e). The prior recoil of IPh away from I-atom(#1) (Figure 1c) ensures that the Ph′ has no secondary encounter with I-atom(#1).

dx.doi.org/10.1021/ja301608q | J. Am. Chem. Soc. 2012, 134, 9320−9326

Threshold Voltages and Current Dependence of the Reaction. The measured threshold value, as in earlier work,[22] corresponds to a peak in the projected density of states (pDOS) plot. For the second C−I bond, the peak is at 1.8 eV, with its onset at +1.6 eV. The unoccupied states are localized around the C−I bond in the IPh residue (see Supporting Information), suggesting excitation of the C−I bond to a negative ion state.

The first bond-breaking was a single-electron process.[22] An electron order of 0.5 is shown in Figure 2b for the second bond-breaking; the error bars do not admit of an order of one. This fractional order may be due to single-electron excitation in competition with an opposing effect. As the current increases, the tunneling gap decreases, with a corresponding increase in electric field. A field gradient is known to decrease the lifetime of an ionic state.[42] This shortened lifetime may be the factor operating in opposition to increased rate at increased current.

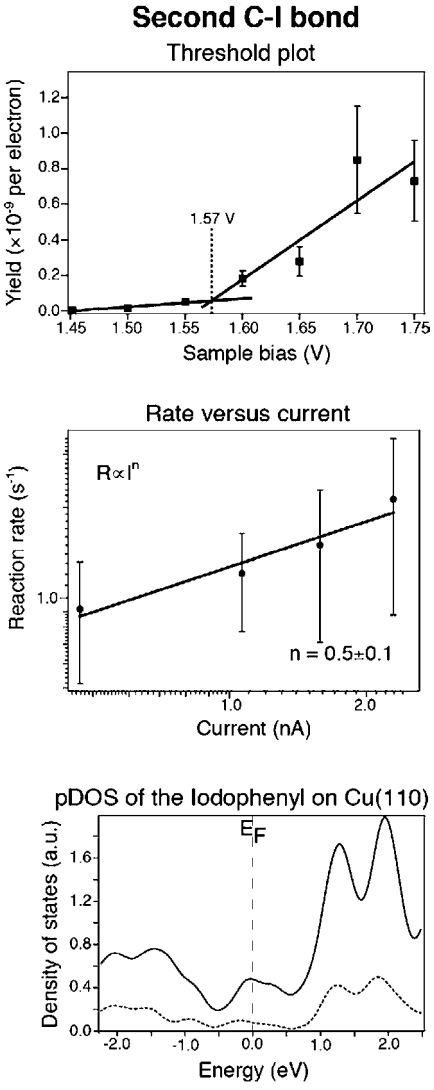

Figure 2. Electron-induced dissociation of the C−I bond in iodophenyl (IPh) bound to the surface. (a) The threshold for this reaction was measured to be 1.57 V, assuming a linear threshold law. Error bars give the standard deviation. (b) The kinetics indicate that the C−I bond break occurs via a half-electron process. Error bars give the standard deviation. (c) The pDOS of the IPh is represented by a solid curve and pDOS of the I-atom by a dashed curve.

The reason it is marked for the second C−I bond-breaking but not the first could lie in the fact that the IPh which embodies the second C−I is chemisorbed on the copper and hence strongly coupled to it.

Theoretical Model for Electron-Induced Reaction. We have modeled the electron-induced reaction of the pDIB on Cu(110) using DFT-based MD . The electron-induced reaction of the first C−I bond was modeled using an ab initio ground-state potential comprising a five-layer copper slab (see Methods) and a similar ionic potential, PES*, but with added negative charge totaling one electron in the antibonding orbitals of the two C−I bonds. This was obtained using an ionic pseudopotential for the I-atoms, placing additional negative charge in their valence shells. This added charge was distributed asymmetrically so that a single C−I bond broke in stage one.

Following the idea of Seideman and co-workers[43] the mean lifetime of the excited state was estimated by a non-equilibrium Green's function approach to be ∼10 fs. With 0.8 excess electronic charge at I-atom(#1), hence 0.2 e^- at I-atom(#2), the ionic state was unstable when it was returned to the ground PES after 80 fs. The probability of such a long excited-state residence time is $\sim 10^{-4}$ times the mean residence time obtained by the procedure of Gadzuk.[44] But this represents a high probability compared with the measured electron efficiency of reaction, $\sim 9 \times 10^{-11}$.

MD were performed on PES* and, following the minimum residence time required for subsequent reaction on the ground PES, namely 80 fs, coordinates and momenta were transferred to the ground PES. MD was continued on the ground PES until the products, IPh and I-atom(#1), had moved apart, to reach a stable minimum. The reaction products were found to be IPh displaced to the left along $[00\bar{1}]$ and attached to Cu-2 (see Figure 1c), and I-atom(#1) recoiling to the right along [001] to the first four-fold hollow. This closely resembled experimental pathway B shown in Figure 1. The need for sufficient time in PES* in order for reaction to ensue across the ground PES is evident on examination of Figure 3, which shows that the system must surmount an energy barrier. The probability of longer residence time than 80 fs on PES* decreases exponentially.

The existence of different categories of dynamics across the ground PES can be explained by reaction across more than one negative ionic state, PES*. The observed alternate major path termed A is distinguished from path B (discussed above) by an almost stationary IPh radical. This was modeled by placing a slightly smaller fraction of the unit electronic charge in the pseudopotential of I-atom(#1), namely $0.75e^-$. The minimum time on this modified PES* for subsequent reaction on the ground PES, was found to be 90 fs. The outcome of reaction on this modified PES* was a stationary IPh bound to Cu-1 (Figure 1b). The I-atom(#1) recoiled to the right along [001] to the first four-fold hollow. This outcome, resembling experimental path A, is attributable in the model to the smaller repulsive impulse between IPh and I-atom(#1). It should be noted that IPh encounters several possible C−Cu binding sites along $[00\bar{1}]$, whereas the I-atom(#1) encounters only one I−Cu four-fold hollow.

Path C in the MD could be obtained by adjusting the charge distribution and ionic residence time, for example by placing $0.65e^-$ in I-atom(#1) and employing 130 fs in PES*. Path D was never obtained in any MD simulation, raising the possibility that this minor path is an artifact due to the interaction between the STM tip and the products.

dx.doi.org/10.1021/ja301608q | J. Am. Chem. Soc. 2012, 134, 9320−9326

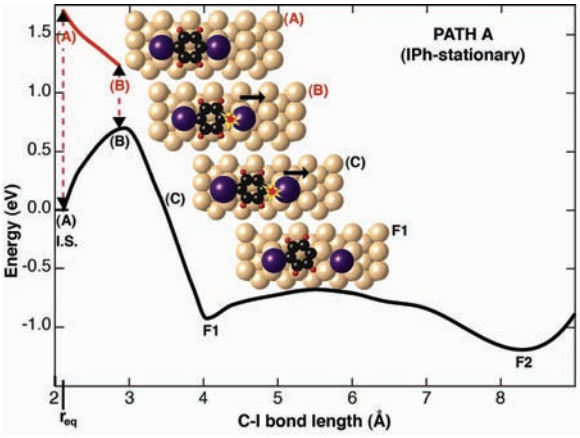

Figure 3. Minimum energy pathway for the electron-induced dissociation of the first C−I bond. At the equilibrium position the pDIB molecule is excited to an ionic pseudopotential in the same geometry as that of the ground state. After a minimum residence time (90 fs for path A) on the PES* the system is returned to the ground PES. The MD is continued on the ground PES until the products have reached a stable minimum (F1).

Similarly, we have modeled the electron-induced reaction of the second C−I bond for paths A and B (see Methods). For path A, a secondary collision was clearly evidenced in theory as in experiment. Details of the computed dynamics are shown in Figure 4. In path B, the first C−I bond-breaking caused the IPh to recoil substantially away from I-atom(#1). The second-bond-breaking with this as its starting point, designated path B′, does not result in a secondary encounter with I-atom(#1) which is distant. This too accords with the experimental finding for second-bond-breaking by path B′.

As a result of these dynamics both pathways A→A′ and B→B′ give the same final increase in distance of 7.2 Å between the two I-atoms at the Cu(110) surface, as reported for two-bond-breaking in pDIB in our preliminary study.[22] Figure 1 shows for the first time the components of this overall separation of the two chemisorbed I-atoms, #1 and #2. For path A→A′ the motions are 1.8 + 3.6 Å for I-atom(#1) and 1.8 Å for I-atom(#2) totaling 7.2 Å. For path B→B′ the component motions are 1.8 Å for I-atom(#1) and 2.7 + 2.7 Å for I-atom(#2), once again totaling 7.2 Å. This breakdown into the stages of I-atom separation is evident in both the experiment and theory reported here.

CONCLUSION

Electron-induced reaction of *p*-diiodobenzene (pDIB) on Cu(110) at 4.6 K is shown by STM to involve the successive breaking of the two C−I bonds. This was modeled by DFT-based two-state MD simulation.

The reagent molecule is initially aligned along the [001] axis of the copper, with its terminal I-atoms on short-bridge (S) sites. All reaction products, namely I-atoms #1 and #2, iodophenyl (Iph) and phenylene (Ph′), were distinguishable as to nature and location, with the assistance of theoretical simulation of the images. All were found to chemisorb in close proximity—typically to within half a lattice spacing—of the parent molecule or radical from which they derived. Thus, "localization" of reaction for successive C−I bond-breaking in pDIB, at a metal surface, was clearly demonstrated.

We identified two major pathways for the release of I-atom(#1). In the more probable (path A, 50% of 117 cases),

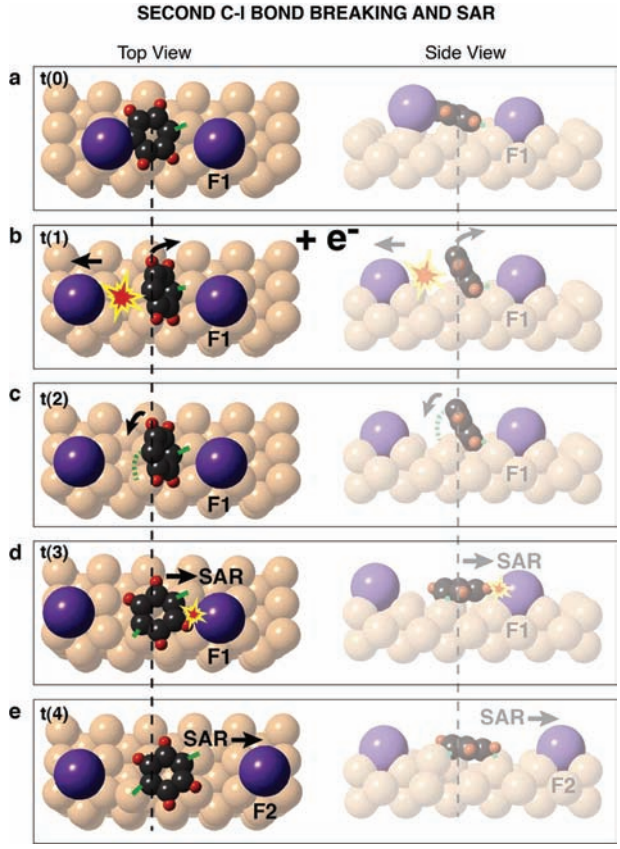

Figure 4. Second C−I bond-breaking and "surface-aligned reaction" (SAR). (a) The initial state for second-bond-breaking is identical to that shown in Figure 1b. (b) Electron-induced dissociation of the IPh residue results in the breaking of the second C−I bond so that I-atom(#2) recoils to the left, and the Ph′ residue turns to the right (bond to surface shown in green). (c) The Ph′ residue forms a second chemisorbed bond to the Cu surface (dashed green). (d) As the second C−Cu bond between the Ph′ and the surface is formed, the Ph′ shifts toward I-atom(#1) severing the I−Cu bond at F1 and forming a new I−Cu bond at F2 in the SAR. (e) Final state consisting of two I-atoms along the [001] direction, separated by 14.4 Å.[22]

the IPh radical remained almost stationary, and I-atom(#1) recoiled strongly to the first and the second four-fold hollow (F1 and F2) along [001]. In a less probable mechanism (path B, 33% of the cases), the IPh recoiled 2.7 Å along $[00\bar{1}]$ and I-atom(#1) recoiled with less momentum along [001], chemisorbing almost exclusively in F1.

The recoil of the products, I-atom(#1) and I-atom(#2), was in opposite directions ([001] and $[00\bar{1}]$). This recoil was marked not only by the short distance that the I-atoms traveled—the "localization" of reaction noted above—but also by the strong *directionality* of their motion. Their direction of motion was collinear with the original I···I axis of the physisorbed pDIB reagent. The recoil of IPh in path B (see above) was directed along $[00\bar{1}]$. Motion of Ph′ was along [001] (see below). These dynamics were successfully modeled using a DFT-based slab model for the ground PES followed by transition to a negatively charged ionic state. This excited state was obtained in a novel fashion employing pseudopotentials to place additional charge in the valence shells of the I-atoms. After a set residence time in the ionic state the system was returned to the ground state where the dynamics proceeded to the products.

dx.doi.org/10.1021/ja301608q | J. Am. Chem. Soc. 2012, 134, 9320−9326

These dynamics, embodying both localization and directionality collinear with the C−I axes, are conducive to secondary encounters, since the reacting species are constrained to one dimension. A clear example of such a secondary encounter was the observation of a substantial (3.6 Å, one lattice spacing) recoil of I-atom(#1) along [001] as a secondary consequence of the release of I-atom(#2) in the opposite direction. The STM image of this event indicates that the Ph′ left behind by the separation of I-atom(#2) from IPh, in the course of attaching to the copper surface, moved along [001] to encounter I-atom(#1) in F1. The secondary collision, Ph′ + I-atom(#1), severed I-atom(#1)'s bond to the surface at F1 and caused the formation of a new bond at the second four-fold hollow farther along [001], i.e., at F2. This aligned secondary encounter to break an I−Cu bond and form a new one along the continuation of the direction of the collision was observed in all 20 instances of path A′. Both the directionality and the efficiency suggest that this is a case of "surface-aligned reaction" (SAR), evidenced at the atomic level.

Molecular dynamics calculations give insight into the localization of reaction, the directionality due to change of the C−I bond into a coaxial antibond, and SAR due to a low-impact-parameter collision between Ph′ and I-atom(#1). In future work we shall compare the recoil distance, and also the directionality along the prior bond-axis, in reactions giving rise to other recoiling atoms. We shall also change the nature of the organic moiety from which the atom recoils (e.g., replacing the benzene ring with biphenyl, or with an alkane chain). We speculate that the reaction dynamics will be governed by (i) the magnitude of the repulsive force acting between the separating fragments, (ii) the effective mass of the recoiling species (their actual mass together with their binding energy to the surface), and (iii) the efficiency of energy transfer from the recoiling species to the surface. All three factors merit investigation.

■ ASSOCIATED CONTENT

Supporting Information

Theoretical details of calculations for the adsorption energy, molecular orbitals, figure showing the minor pathways C and D, and figure showing a large area for the major pathway. This material is available free of charge via the Internet at http://pubs.acs.org.

■ AUTHOR INFORMATION

Corresponding Author

jpolanyi@chem.utoronto.ca

Notes

The authors declare no competing financial interest.

■ ACKNOWLEDGMENTS

We thank J. Tully and P. Saalfrank for critical comments on the theoretical model. This work was funded in part by the Natural Sciences and Engineering Research Council of Canada (NSERC), the Xerox Research Centre Canada (XRCC), and the Canadian Institute for Advanced Research (CIFAR). We are grateful to I. R. McNab for many helpful discussions. Computations were performed on TCS at SciNet HPC Consortium funded by the Canada Foundation for Innovation.

■ REFERENCES

(1) Hla, S.-W.; Meyer, G.; Rieder, K.-H. *Chem. Phys. Chem.* **2001**, *2*, 361−366.
(2) Hla, S.-W.; Meyer, G.; Rieder, K.-H. *Chem. Phys. Lett.* **2003**, *370*, 431−436.
(3) Ho, W. *J. Chem. Phys.* **2002**, *117*, 11033−11061.
(4) McNab, I. R.; Polanyi, J. C. *Chem. Rev.* **2006**, *106*, 4321−4354.
(5) Lu, P. H.; Polanyi, J. C.; Rogers, D. *J. Chem. Phys.* **1999**, *111*, 9905−9907.
(6) Lu, P. H.; Polanyi, J. C.; Rogers, D. *J. Chem. Phys.* **2000**, *112*, 11005−11010.
(7) Dobrin, S.; Harikumar, K. R.; Polanyi, J. C. *Surf. Sci.* **2004**, *561*, 11−24.
(8) Harikumar, K. R.; Petsalakis, I. D.; Polanyi, J. C.; Theodorakopoulos, G. *Surf. Sci.* **2004**, *572*, 162−178.
(9) Dobrin, S.; Lu, X.; Naumkin, F. Y.; Polanyi, J. C.; Yang, S. Y. *Surf. Sci.* **2004**, *573*, L363−L368.
(10) Harikumar, K. R.; McNab, I. R.; Polanyi, J. C.; Zabet-Khousousi, A.; Hofer, W. A. *Proc. Natl. Acad. Sci. U.S.A.* **2011**, *108*, 950−955.
(11) Harikumar, K. R.; Leung, L.; McNab, I. R.; Polanyi, J. C.; Lin, H.; Hofer, W. A. *Nature Chem.* **2009**, *1*, 716−721.
(12) Dobrin, S.; Harikumar, K. R.; Matta, C. F.; Polanyi, J. C. *Surf. Sci.* **2005**, *580*, 39−50.
(13) Sloan, P. A.; Palmer, R. E. *Nature* **2005**, *434*, 367−371.
(14) Sakulsermsuk, S.; Sloan, P. A.; Palmer, R. E. *ACS Nano* **2010**, *4*, 7344−7348.
(15) Ullmann, F.; Meyer, G. M.; Loewenthal, O.; Gilli, E. *Justus Leibigs Ann. Chem.* **1904**, *332*, 38−81.
(16) Hla, S.-W.; Bartels, L.; Meyer, G.; Rieder, K.-H. *Phys. Rev. Lett.* **2000**, *85*, 2777−2780.
(17) McCarty, G. S.; Weiss, P. S. *J. Phys. Chem. B* **2002**, *106*, 8005−8008.
(18) McCarty, G. S.; Weiss, P. S. *J. Am. Chem. Soc.* **2004**, *126*, 16772−16776.
(19) Lipton-Duffin, J. A.; Ivasenko, O.; Perepichka, D. F.; Rosei, F. *Small* **2009**, *5*, 592−597.
(20) Dougherty, D. B.; Lee, J.; Yates, J. T., Jr. *J. Phys. Chem. B* **2006**, *110*, 20077−20080.
(21) Maksymovych, P.; Yates, J. T., Jr. *J. Am. Chem. Soc.* **2006**, *128*, 10642−10643.
(22) Leung, L.; Lim, T.; Polanyi, J. C.; Hofer, W. A. *Nano Lett.* **2011**, *11*, 4113−4117.
(23) Bourdon, E. B. D.; Das, P.; Harrison, I.; Polanyi, J. C.; Segner, J.; Stanners, C. D.; Williams, R. J.; Young, P. A. *Faraday Discuss. Chem. Soc.* **1986**, *82*, 343−358.
(24) Polanyi, J. C.; Williams, R. J. *J. Chem. Phys.* **1988**, *88*, 3363−3371.
(25) Mieher, W. D.; Ho, W. *J. Chem. Phys.* **1989**, *91*, 2755−2756.
(26) Mieher, W. D.; Ho, W. *J. Chem. Phys.* **1990**, *92*, 5162−5163.
(27) Chakarov, D. V.; Ho, W. *J. Chem. Phys.* **1991**, *94*, 4075−4077.
(28) Mieher, W. D.; Ho, W. *J. Chem. Phys.* **1993**, *99*, 9279−9295.
(29) Yamanaka, T.; Inoue, Y.; Matsushima, T. *Chem. Phys. Lett.* **1997**, *264*, 180−185.
(30) Yamanaka, T.; Inoue, Y.; Matsushima, T. *J. Chem. Phys.* **1999**, *110*, 2597−2605.
(31) Setzler, J. V.; Guo, H.; Schatz, G. C. *J. Phys. Chem. B* **1997**, *101*, 5352−5361.
(32) Setzler, J. V.; Bechtel, J.; Guo, H.; Schatz, G. C. *J. Chem. Phys. B* **1997**, *107*, 9176−9184.
(33) Tripa, C.; Yates, J. T., Jr. *Nature* **1999**, *398*, 591−593.
(34) Tripa, C. E.; Yates, J. T., Jr. *J. Chem. Phys.* **2000**, *112*, 2463−2469.
(35) Vaida, M. E.; Bernhardt, T. M. *ChemPhysChem* **2010**, *11*, 804−807.
(36) Kresse, G.; Furthmuller, J. *Phys. Rev. B* **1996**, *54*, 11169−11186.
(37) Grimme, S. *J. Comput. Chem.* **2004**, *25*, 1463−1475.
(38) Perdew, J. P.; Ernzerhof, M.; Burke, K. *J. Chem. Phys.* **1996**, *105*, 9982−9985.
(39) Palotás, K.; Hofer, W. A. *J. Phys.: Condens. Matter* **2005**, *17*, 2705−2713.
(40) Kresse, G.; Joubert, D. *Phys. Rev. B* **1999**, *59*, 1758−1775.
(41) Köhler, L.; Kresse, G. *Phys. Rev. B* **2004**, *70*, 165405.

(42) Simmons, J. Molecular Anions, www.hec.utah.edu/anions (accessed Nov 4, 2011).
(43) Yoder, N. L.; Guisinger, N. P.; Hersam, M. C.; Jorn, R.; Kaun, C.-C.; Seideman, T. *Phys. Rev. Lett.* **2006**, *97*, 187601.
(44) Gadzuk, J. W. *Phys. Rev. B* **1991**, *44*, 13466−13477.